UDC 621.34-52

M. Pechenik, O. Kiselychnyk, Ph.Ds, Ukraine
S. Buryan, D. Petukhova Kiev
National Technical University of Ukraine "Kiev Polytechnic Institute"

SENSORLESS CONTROL OF WATER SUPPLY PUMP BASED ON NEURAL NETWORK ESTIMATION

Expediency of application of artificial neural networks for estimation of water supply pump flow rate and head is shown. A design procedure of a water head neural network estimator is considered. A hybrid model of the pump affording research of the estimation and sensor free control processes is developed. Simulation results of the processes of water head sensor free stabilization are presented

Показано доцільність застосування апарату штучних нейронних мереж для оцінювання продуктивності та напору помп водопостачання. Розглянуто процедуру розробки нейроестіматора напору. Розроблено гібридну модель помпової установки, придатну для дослідження процесів оцінювання та бездатчикового керування. Наведено результати симулювання процесів бездатчикової стабілізації напору.

Показана целесообразность использования аппарата искусственных нейронных сетей для оценивания производительности и напора насосов водоснабжения. Рассмотрена процедура разработки нейроэстиматора напора. Разработана гибридная модель насосной установки, позволяющая исследовать процессы оценивания и бездатчикового управления. Наведены результаты симулирования процессов бездатчиковой стабилизации напора.

1. Introduction

Research and development of energy and resources saving technologies in the domain of water supply systems is very important for all countries. The best results are achieved there with the implementation of a controlled induction motor drive as a pump mover and an energy-efficient control and automation algorithm based on modern control theory [6]. Pump head stabilization system and water demand predictors combining with pump scheduling have found the most widespread application in practice. Recently the leading manufacturers of pumps also propose so-called intelligent pumps controlling both the pump and the motor and providing many functions for energy saving, and reliable operation. An interesting example is the Grundfoss Magna pump's ability to meet system demand at the lowest possible control curve, thus maximizing energy saving [6]. A new direction of research, so-called "interactive" control, also started recently exploiting an interplay between the control law and the consumers response [3,5,7]. It automatically searches for the lowest pump velocity that satisfies consumers' demand. Extremal control systems searching for pump's operating points with maximum efficiency are also developed for parallel and series connection of pumps [8].

The main drawback of the existing systems becomes apparent for small scale water supply systems. In this case, the costs of the head or flow rate sensors are about the same as the cost of the pump and the induction motor together. This fact directed the efforts of researchers on the development of sensorless control systems (without head or flow rate sensors).

The idea of the sensorless control of centrifugal pump bases on the fact that any pump's operating point for any velocity on the head-flow rate steady-state characteristic corresponds to a unique point on the pump's shaft power-flow rate characteristic. Therefore, knowing of the pump velocity and measuring the consumed active power at the terminals of the driving induction motor gives possibility to compute the values of the head and flow rate from the characteristics addressed above. Note that the consumed active power differs from the pump's shaft power by the value of electric drive's losses causing estimation errors. Manufactures embed a number of the characteristics in the memory of the frequency converters combining functions of pump and motor control. The approach is sufficient for systems with a slow change of hydraulic resistance. The most known products are Danfoss VLT® AQUA Drive and Vogelpumpen Hydrovar [6]. A description of the method of sensorless pump control based on measurements of stator voltages and currents of the pump induction motor utilizing extended Kalman filter estimation is presented in [4]. It is more complicated and recommended for systems with fast dynamics.

The objective of the paper is to show expediency of application of the neural network estimation of the head and flow rate. Another task is to develop a procedure of design, simulation and research of the sensorless head stabilization system.

2. Expediency of application of the neural network estimation of the head and flow rate

A centrifugal pump Calpeda MXH 202E with the rated power 0.33 KW equipped with a three phase squirrel cage induction motor with rated 2900 rpm and 220 V phase voltage was researched. A frequency convertor Lenze 8200 Vector with the rated power 0.75KW fed the stator winding of the motor. During the experiments, the convertor provided the constant ratio of the stator voltage amplitude and square of the stator voltage frequency. The head and flow rate were measured by the corresponding sensors MBS3000 and Kobold DRS1.15 connected to digital ammeters with an internal 24 V DC source, while the consumed power (active power at the stator terminals) and frequency were measured by the monitoring system of the convertor.

Fig.1 demonstrates the experimental steady-state dependences of the water head on the flow rate for different voltage frequencies. The experimental points are marked as asterisks. A well-known approximation of the dependence of the head on the flow rate is as follows [4]

$$H = H_{0r}(\omega/\omega_r)^2 - a_p Q^2, \qquad (1)$$

where H and Q denote pump's head and flow rate respectively, ω is the pump velocity, H_{0r} is the head of the pump with zero flow rate and rated velocity ω_r, and a_p is a hydraulic resistance of the pump.

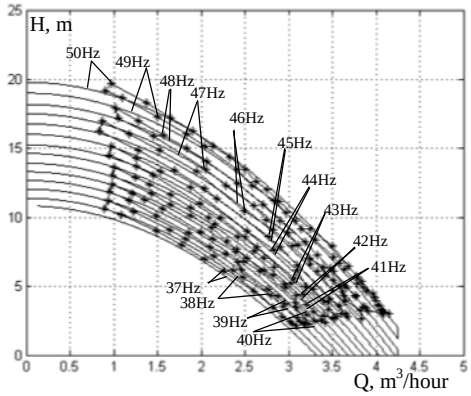

Fig.1. The dependence of the head on the flow rate for different frequencies

Since during the experiments, the frequency f was measured instead of the velocity than the experimental curves on Fig. 1 could be approximated by similar expression

$$H = H_{0r}(f/f_r)^2 - a_p Q^2. \qquad (2)$$

where f_r is the rated frequency.

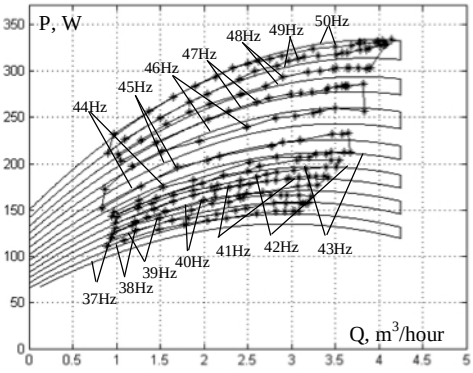

Fig.2. The dependence of the consumed power on the flow rate for different frequencies

The values of H_{0r} and a_p were computed from the rated experimental characteristic in such a way that the rated experimental and approximated characteristics had two joint points. The approximated characteristics for other frequencies were determined using the same computed values of H_{0r} and a_p (see the curves without asterisks). As it is seen from Fig. 1, the quality of approximation is acceptable in the working range of operating points.

Fig. 2 shows the corresponding experimental dependences of the consumed active power on the flow rate. The experimental points are also marked with asterisks. The widespread approximation of the pump power versus the flow rate is [4]

$$P = a(\omega/\omega_r)^3 + b(\omega/\omega_r)^2 Q + c(\omega/\omega_r)Q^2. \qquad (3)$$

where a, b, and c are constants for a specific pump.

The approximations presented in Fig. 2 (the curves without asterisks) were taken similar

$$P = a(f/f_r)^3 + b(f/f_r)^2 Q + c(f/f_r)Q^2. \qquad (4)$$

The approximation coefficients a, b, and c were derived from the rated experimental dependence in order to the rated experimental and approximated characteristics had three joint points. The same values were used during the computation of the curves for other frequencies. The deviation of the corresponding experimental and approximated characteristics is not acceptable to be used for flow rate (and following head) estimation based on frequency and active power measurement. More over, the approximation at lower frequencies gives regions where the power reduces with the flow rate increase. Physically, it is not possible. One way to overcome the problem is to determine the separate approximation coefficients for each characteristic and to exclude the "incorrect" regions. But this complicates the implementation of the estimation. In the same time, the accuracy of the estimation highly depends on the number of characteristics embedded in the memory of the controller. A more simple and effective solution is implementation of a neural network for the head and flow rate estimation. In this case, the approximation is a result of neural network learning based on the experimental data. It allows estimating precisely the values of the head and flow rate even for the operating points between the experimental characteristics. Note that the pump's shaft power is also eliminated from the estimation algorithm.

3. Design of the neural network head estimator

Since the neural network determines the dependence between its input and output vectors, the output vector (the target of learning) is an array of the experimental values of the head or flow rate for the corresponding estimators respectively. The input vector is a matrix comprising two arrays of the experimental values of the consumed active power and frequency (or velocity, if it is measured instead of the frequency) corresponding to the head and flow rate. Note that the steady-state velocity of the induction motor is a function of the frequency (and the voltage amplitude tied to the frequency) and a load torque (the pump's shaft power divided by the velocity). Therefore, there is no matter what is used for the estimation: the frequency or the velocity.

A neural network of the feed-forward backpropagation type is chosen for the estimator implementation. The network includes three layers with 7, 20, and 1 neurons in the first, second and third layers respectively. The tansig activation functions are chosen in the first and second layers, and the purelin function is utilized for the third one. The training function is trainlm. Fig. 3 shows a comparison of the experimental dependences of the head on the frequency and consumed active power and the dependences of the output of the network (the estimated value of the head) on its input vector (the experimental

values of the frequency and the power) computed during simulation. In the researched ranges of frequencies and powers, the estimation of the head is acceptable for the control purpose. Similar results can also be easily obtained for the flow rate estimator. To decrease the number of neurons and provide the same quality of the estimation is necessary to increase the number of experimental points.

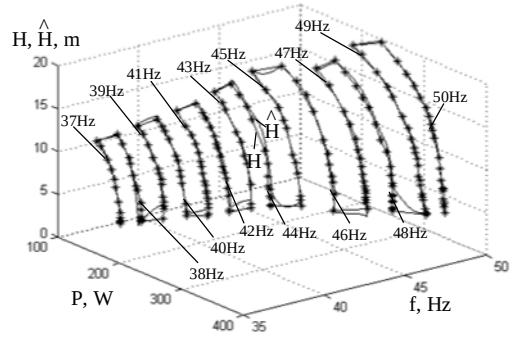

Fig.3. Comparison of the experimental head and the estimated value

Note that in the case of the analytical approximation, the estimation of the head is performed based on the estimation of the flow rate. The neural network head and flow rate estimators deal only with measured or referred values. For example, the frequency convertor Lenze 8200 Vector two analogous outputs can be adjusted in such a way that the voltages there are proportional to the frequency and consumed active power. They can be easily read by a microcontroller with ADCs and then processed according to the neural network estimator's mathematical description. The output signal should be calibrated within 4-20 mA for the standard connection to the feedback input of the Lenze 8200 converter's embedded PID controller.

4. The hybrid model of the centrifugal pump

A typical model of the centrifugal pump with the frequency controlled induction motor drive is presented in [4]. Specifically, the pump flow rate dynamics is described by a non-linear differential equation of the first order

$$\frac{dQ}{dt} = \frac{H_{0r}}{\chi_p \omega_r^2}\omega^2 - \frac{1}{\chi_p}H_{ST} - \frac{1}{\chi_p}(a_n + a_p)Q^2, \qquad (5)$$

where H_{ST} is the height of water lifting, a_n is the hydraulic resistance of the network, χ_p is the integration constant.

Equation (5) is valid if the back vent at the pump's output is opened (if $Q > 0$). In the opposite case (if $Q \le 0$), Q is set to zero.

The value of the pump head H is computed from (1). The value of the pump's shaft power [4] can be determined as follows

$$P_p = \rho g Q H / \eta, \qquad (6)$$

where ρ is the water density, g is the constant of gravity, and η is the pump efficiency.

The pump efficiency η is a function of the head and the flow rate $\eta = f(Q,H)$. In many cases, the control range of the pump's flow rate and head is limited and the pump's efficiency can be considered a constant. Alternatively, the pump's shaft power can be approximated by an equation similar to (3) [4].

The load torque of the pump's motor is

$$T_L = P_p / \omega. \qquad (7)$$

Since the case of the estimation based on the measurement of the consumed active power is developed then the shaft power P_p should be replaced by the consumed power in the pump's model. It is implemented by adding into the model a neural network estimator of the consumed active power with the input vector based on the experimental values of the flow rate and head. The same structure of the estimator as for the case of the head estimation is chosen. Fig. 4 shows the output of the consumed active power estimator and the experimental values corresponding to the experimental values of the flow rate and head.

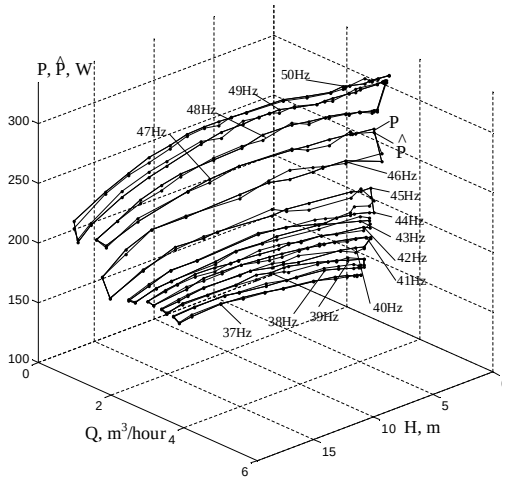

Fig.4. Comparison of the experimental consumed active power and the estimated value

Since the accuracy of approximation (2) is acceptable then equations (1) and (5) are left and combined with the consumed active power estimator in the pump model. Note that the model includes the internal estimator not used in the sensorless control algorithm. It is only utilized for simulation purpose. This is the reason we call this model as a "hybrid" model of the pump.

The model also comprises the well-known two-phase model of the induction motor in the stator reference frame a-b [4]. To compute the load torque the pump's shaft power is determined as the difference between the consumed active power and power losses in the induction motor. The general power losses include the copper and steel losses and the mechanical losses as well [1]. For the simplification purpose, the copper losses are only accounted during the simulation according to the equation

$$\Delta P_c \approx \frac{3}{2}\left[\left(i_{1a}^2 + i_{1b}^2\right)R_1 + \left(i_{2a}^2 + i_{2b}^2\right)R_2\right]. \qquad (8)$$

where i_{1a}, i_{1b} are the stator currents, i_{2a}, i_{2b} are the rotor currents, R_1, R_2 denote the stator and rotor resistances.

The block diagram of the frequency convertor used in the model is presented in Fig. 5. The following notation is accepted: U_{1a}, U_{1b} are the stator voltages, Θ is the electric angle, U_m is the amplitude of the stator voltage,

T_μ is a small time constant, U_{mr} is the rated value of U_m, U_0 is the voltage amplitude at zero frequency, U_m^* is the reference of U_m, f^* is the referred frequency, $k = (U_{mr} - U_0)/f_r^2$.

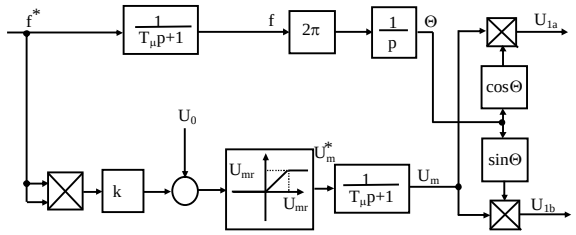

Fig.5. Block diagram of the frequency convertor

The hybrid model of the pump with the frequency controlled induction motor drive is depicted in Fig. 6, where P marked with "^" denotes the estimate of the consumed active power.

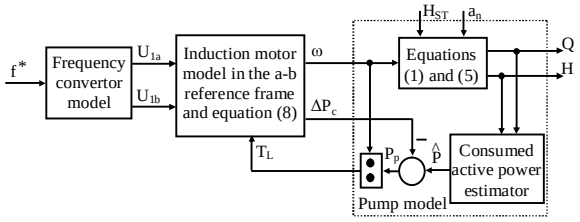

Fig.6. The block diagram of the pump hybrid model

5. The block diagram of the sensorless head stabilization system

The block diagram of the sensorless head stabilization system is presented in Fig. 7, where H marked with "^" denotes the estimate of the head, and $W_{HC}(p)$ is the transfer function of the head controller. Although the embedded PID controller of the frequency converter is discrete, the continuous transfer function can be used because the sample time is very small and enough to consider the discrete control system as a continuous one.

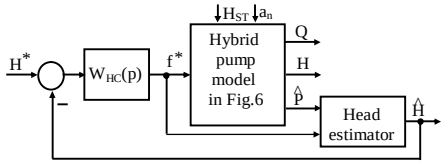

Fig. 7. The block diagram of the sensorless head stabilization system

To compute the parameters of the PID controller develop a linearized model of the system. Consider a small perturbation of the velocity $\delta\omega$ causing a small perturbation of the flow rate δQ in equation (5). The difference of equation (5) with the substitutions $\omega = \omega_{op} + \delta\omega$, $Q = Q_{op} + \delta Q$, where index "op" denotes an equilibrium operating point, and equation (5) for the equilibrium with the substitutions $\omega = \omega_{op}$, $Q = Q_{op}$, and neglecting second-order terms results in

$$\delta Q \quad \frac{k_q}{T_q p + 1}\delta\omega, \qquad (9)$$

where $k_q = H_{0r}\omega_{op}/(\omega_r^2 Q_{op}(a_n + a_p))$ and the time constant $T_q = \chi_p/(2Q_{op}(a_n + a_p))$.

Similar manipulation applied to equation (1) gives

$$\delta Q \quad \frac{H_{0r}\omega_{op}}{\omega_r^2 a_p Q_{op}}\delta\omega - \frac{1}{2a_p Q_{op}}\delta H. \qquad (10)$$

With substitution (10) into (9), one obtains

$$\delta H \quad k_h \frac{T_h p + 1}{T_q p + 1}\delta\omega, \qquad (11)$$

where $k_h = 2H_{0r}\omega_{op}a_n/(\omega_r^2(a_n + a_p))$ and the time constant $T_h = T_q(1 + a_p/a_n)$.

A simplified linearized model of the frequency controlled induction motor drive [2] neglecting the electromagnetic transients can be written as

$$\delta\omega \quad \frac{2\pi/p_n}{T_M p + 1}\delta f^*, \qquad (12)$$

where p_n is the number of the motor poles, T_M is the electromechanical time constant.

The transfer function of the open head loop without the head controller assuming no head estimation error

$$W_{ohl}(p) = \frac{2k_h\pi/p_n}{T_M p + 1}\frac{T_h p + 1}{T_q p + 1}. \qquad (13)$$

The standard adjustment providing 4.3% overshooting gives the following head controller

$$W_{HC}(p) = \frac{W_{ohl}^{-1}(p)}{2T_M p(T_M p + 1)} = k_{HC}\frac{T_{HC}p + 1}{T_{HC}p}\frac{1}{T_h p + 1}, \qquad (14)$$

where $k_{HC} = p_n T_q/(4\pi T_M k_h)$, $T_{HC} = T_q$.

It is a series connection of a PI-controller and a filter. In case of the industrial frequency converter, the implementation requires additional equipment for the filter. A simpler way is to leave only the PI-controller and to choose the acceptable parameters of the controller during the simulation of the nonlinear system.

6. Simulation of the sensorless head stabilization system

The following values of the motor and convertor parameters were used during the simulation R_1 =32.892 Ω, R_2 =22.555 Ω, the stator and rotor inductances L_1 =1.9095 H, L_2 =1.9304 H, the mutual inductance of the stator and rotor L_{12} = 1.8706 H, p_n =1, the inertia J =0.048 kgm^2, T_μ =0.001 s, U_{mr} =310 V, U_0 =0.06U_{mr}, f_r =50 Hz. The following parameters of the pump model were utilized a_p =1.534·10^7 s^2/m^5, χ_p =1.5 s·hour/m^2, H_{ST} =1 m. Fig. 8 shows the estimation process during a start of the open loop system (Fig. 6) and changes of the hydraulic resistance of the network. The value of the estimation error during the simulation is mainly caused by accounting not all power losses in the motor model. During the start, the reason of the error is also the values of the input vector of the estimator beyond the learning ranges. The step response of the stabilization system using the head estimate as a feedback is depicted in Fig. 9.

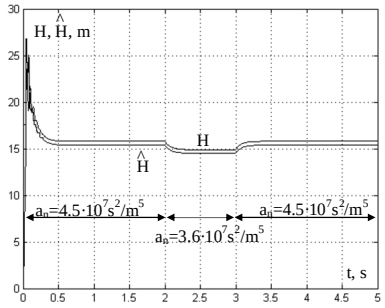

Fig.8. The estimation process in the open loop system

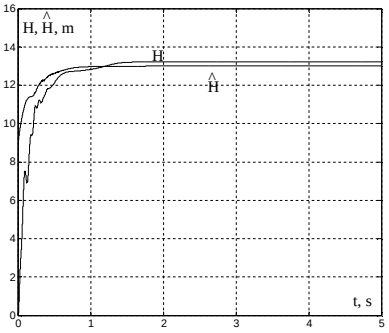

Fig. 9. The estimation process in the stabilization system

7. Conclusions

The neural network estimation of the pump head and flow rate is a good alternative to the estimation based on analytical approximation. It allows to increase the accuracy of estimation. Simulation of the sensorless head stabilization system requires development of the "hybrid" model with the estimation of the consumed active power.

References

1. Екстремальні енергозберігаючі електромеханічні системи з асинхронним електроприводом/ М.Г.Попович, М.В.Печеник, О.В.Ковальчук, О.І.Кіселичник// Вісн. нац. техн. ун-ту "Харківський політехнічний інститут". – 2001. – № 10. – С.314-318.

2. Особливості синтезу та дослідження електромеханічних систем з послідовною корекцією та частотно регульованими асинхронними двигунами / М.Г. Попович, В.І.Теряєв, О.І.Кіселичник, С.О.Бур'ян // Вісн. Кременч. держ. політехн. ун-ту ім. М. Остроградського. – 2007. – № 3 (44).– Ч. 2. – С.12-16.

3.Improved interactive energy saving control algorithms of water supply pump based on head measurement / O.Kiselychnyk, S.Buryan, M.Bodson, H.Werner // Problems of automated electric drive. "Electroinform".– Lviv:– 2009. – P.349-354.

4. Kiselychnyk O.I. Nonsensor control of centrifugal water pump with asynchronous electric-drive motor based on extended Kalman filter/ O. I. Kiselichnik, M. Bodson// Russian Electrical Engineering. – 2011. – Vol. 82, N. 2. – P. 69–75. Allerton Press, Inc., USA.

5. Kiselychnyk O. Interactive energy saving control of water supply pump based on pressure measurement/ O. Kiselychnyk, M. Bodson, H. Werner// Transactions of Kremenchuk State Polytechnic University. – 2009. – N. 3 (56), part 1. – P. 166–171.

6. Kiselychnyk O. Overview of energy efficient control solutions for water supply systems/ O. Kiselychnyk, M. Bodson, H. Werner// Transactions of Kremenchuk State Polytechnic University. – 2009. – N. 3 (56), part 1. – P. 40–45.

7. Pechenik M. Experimental research of interactive energy saving controller of water supply pump based on flow rate measurement/ M. Pechenik, O. Kiselychnyk, S. Buryan// Transactions of Kharkiv National Technical University. – 2010. – N.28. – P.272-274.

8. Popovich M. Extremal electromechanical control system of water supply pumps connected in series/ M.Popovich, O.Kiselychnyk, S.Buryan// Transactions of Kremenchuk State University. – 2010. – N3 (62), part 2. – P.37-41.

Received 07.07.2011

Mykola Pechenik,
Ph.D., Professor of the Department of Automation of Electromechanical Systems and Electric Drive of the National Technical University of Ukraine "KPI",
Prospect Peremohy, 37
03056 Kiev, Ukraine
E-mail: pechenik@ntu-kpi.kiev.ua

Oleh Kiselychnyk,
Ph.D., Associate Professor of the Department of Automation of Electromechanical Systems and Electric Drive of the National Technical University of Ukraine "KPI"
Prospect Peremohy, 37
03056 Kiev, Ukraine
E-mail: koi@gala.net

Serhiy Buryan,
Ph.D. student of the Department of Automation of Electromechanical Systems and Electric Drive of the National Technical University of Ukraine "KPI"
Prospect Peremohy, 37
03056 Kiev, Ukraine
E-mail: sburyan@rambler.ru

Dina Petukhova,
Student of the Department of Automation of Electromechanical Systems and Electric Drive of the National Technical University of Ukraine "KPI"
Prospect Peremohy, 37
03056 Kiev, Ukraine
E-mail: eleron@svitonline.com